likely it is that the merger has happened in the exact position of the j-th AGN, and $n_{\mathrm{AGN},j}$ is the number density of the AGN catalogue in the redshift bin where the j-th AGN is. The value of this number density has been calculated for each AGN in all the sub-samples of $\mathrm{Quaia}_{\mathrm{cut}}$ by dividing the total number of objects in every redshift bin by the comoving volume enclosed in such a bin, excluding the region in which $|b| < 10°$. The background probability density is calculated as

$$\mathcal{B}_i = \frac{0.9}{\mathrm{V90}_i} \quad , \tag{5.7}$$

where, in analogy to what has been done in Veronesi et al. (2023b) and in Veronesi et al. (2024), the 0.9 factor ensures that $\mathcal{B}_i$ and $\mathcal{S}_i$ have the same normalisation.

We cross-match the sky maps of the 159 GW events with the 5 different sub-samples of $\mathrm{Quaia}_{\mathrm{cut}}$ separately, using the `postprocess.crossmatch` function of the package `ligo.skymap`. The results of these cross-matches are used to evaluate $\mathcal{L}(f_{\mathrm{AGN}})$. We then calculate the posterior probability distribution $\mathcal{P}_{f_{\mathrm{AGN}}}$, normalising the likelihood function and assuming a uniform prior on f_{AGN} in the $[0, 1]$ range.

5.4 Results

The posterior probability on f_{AGN} peaks at $\hat{f}_{\mathrm{AGN}} = 0$ independently on which sub-set of $\mathrm{Quaia}_{\mathrm{cut}}$ we use for the cross-match. In Figure 5.5 is shown in blue the region of the parameter space investigated in this work that our analysis rejects with a credibility of 95 per cent. We show the comparison with previous results, obtained in Veronesi et al. (2023b) using a more limited dataset.

In Table 5.3 we list, as a function of the threshold on bolometric luminosity, how many objects are considered during the cross-match, what fraction of $\mathrm{Quaia}_{\mathrm{cut}}$ they consist of, and the upper limits we put on f_{AGN} at 68, 90, and 95 per cent credibility.

Figure 5.6 shows the logarithm of the ratio between the single-event likelihood calculated at $f_{\mathrm{AGN}} = 1$ and the one calculated at $f_{\mathrm{AGN}} = 0$, as a function of V90. Different panels correspond to different bolometric luminosity thresholds. In each plot the markers are coloured according to the average completeness inside the localisation volume of the corresponding merger. The dashed horizontal lines indicate where the logarithm has a null value, therefore where $\mathcal{L}_i(f_{\mathrm{AGN}} = 1) = \mathcal{L}_i(f_{\mathrm{AGN}} = 0)$. The markers above the horizontal dashed line

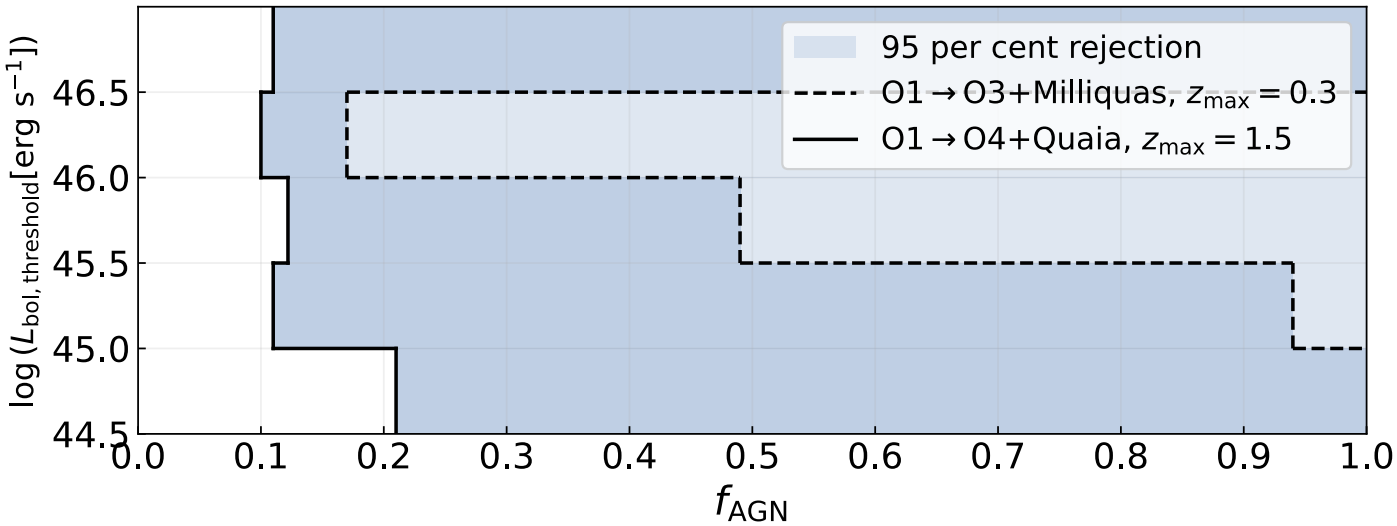

Figure 5.5: Observational constraints on $f_{\rm AGN}$ based on spatial correlation. The blue region of the plot shows the region of the parameter space we investigated that is rejected by our analysis at a 95 per cent credibility level. The region enclosed in in the dashed line shows the results obtained with a more limited dataset in Veronesi et al. (2023b). Such previous work used the 30 GW events detected in the first three observing runs of the LVK collaboration located within $z = 0.3$ at a 90 per cent credibility level, and three different catalogues of AGN in the same redshift range. The region enclosed in the solid line shows the results of this work, which explores a wider range of AGN luminosities and uses all the mergers of binaries of COs directly detected up until June 1st, 2024.

Table 5.3: Upper limits on $f_{\rm AGN}$ we obtain at different levels of credibility, for the three cuts in bolometric luminosity we consider. For each of such cuts we also list the number of AGN used in the analysis ($N_{\rm AGN,\ cut}$), and what fraction of the total number of AGN ($N_{\rm AGN,\ Quaia_{cut}}$) they consist of. All the values in this table have been rounded up to the second decimal digit.

$\log\left(L_{\rm bol,threshold}\ \left[\text{erg s}^{-1}\right]\right)$	$N_{\rm AGN,\ cut}$	$N_{\rm AGN,\ cut}/N_{\rm AGN,\ Quaia_{cut}}$	68 per cent upper limit	90 per cent upper limit	95 per cent upper limit
46.5	20236	0.03	0.05	0.09	0.11
46	177117	0.27	0.04	0.08	0.10
45.5	490628	0.74	0.05	0.10	0.13
45	644393	0.98	0.05	0.09	0.11
44.5	659949	1.00	0.08	0.16	0.21

correspond to GW events according to which the hypothesis of no-correlation between mergers and AGN is disfavoured.

One event in particular, detected during the second half of O4, has a correspondent value of $\mathcal{L}_i\left(f_{\rm AGN}=1\right)/\mathcal{L}_i\left(f_{\rm AGN}=0\right)$ which is greater than one, independently on the luminosity cut of the Quaia sub-sample it is cross-matched with. The ID of such event is S240511i, and the corresponding marker is particularly evident in the first two panels of Figure 5.5. In the case of the cross-match with the sub-sample of $\text{Quaia}_{\rm cut}$ characterised by AGN brighter than $10^(46.5)$erg s^{-1} ($10^(46)$erg s^{-1}), for this particular GW event $\log\left(\mathcal{L}_i\left(f_{\rm AGN}=1\right)/\mathcal{L}_i\left(f_{\rm AGN}=0\right)\right)\approx 1.32$ (0.72), which means that the single-event likelihood calculated at $f_{\rm AGN}=1$ is $\approx$ 21 (5) times larger than at $f_{\rm AGN}=0$. This result based solely on spatial correlation hints towards a possible AGN origin of such event. Further follow-up analyses regarding this merger and its intrinsic binary properties will be needed to be able to draw any definitive conclusion.

5.5 Discussion and conclusion

In this work we present new observational constraints on the fractional contribution of the AGN channel to the total observed merger rate of binaries of COs. These constraints are obtained using the same spatial-correlation-based approach used in (Veronesi et al. 2023b). With respect to our previous work, we make use of a new, larger dataset, which consists of 159 GW events detected by the interferometers of the LVK collaboration not later than June 1st, 2024 and of the all-sky AGN catalogue Quaia. In particular we use all the AGN contained in such a catalogue that have a redshift estimate not larger than $z=1.5$ and an absolute value of the galactic latitude $|b|\geq 10°$. We call this sub-sample $\text{Quaia}_{\rm cut}$.

We estimate the bolometric luminosity of every object in $\text{Quaia}_{\rm cut}$ using the magnitudes in the Gaia $G_{\rm RP}$ band. We also estimate the completeness of such a catalogue as a function of redshift for different values of bolometric luminosity threshold. The average value of the completeness within the 90 per cent Credibility Level localisation volume of each GW event is used during the likelihood maximisation process.

We calculate the posterior probability function on the fractional contribution of the AGN channel to the total merger rate for all the different luminosity thresholds, obtaining that this function always peaks at $\hat{f}_{\rm AGN}=0$. We calculate the upper limits of the 68, 90, and 95 per cent Credibility Intervals on $f_{\rm AGN}$.

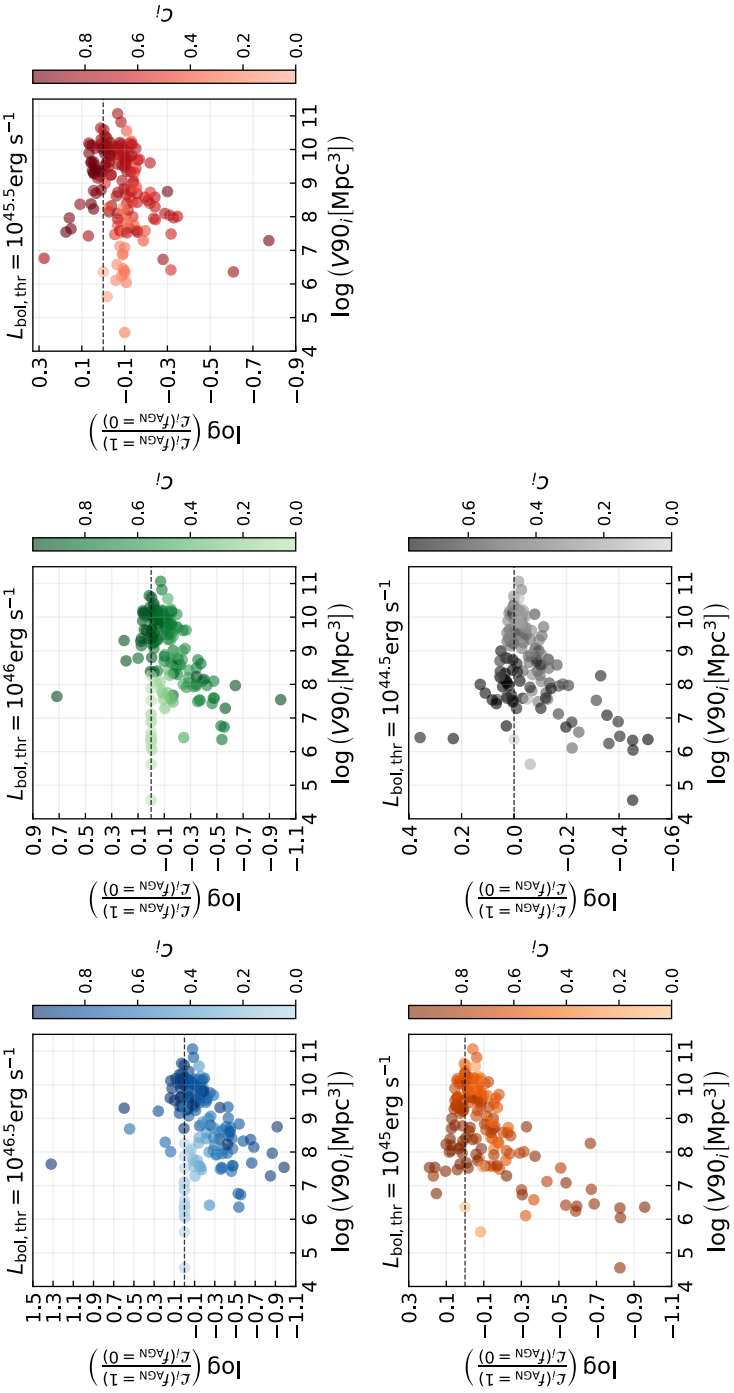

Figure 5.6: Logarithm of the ratio between the value of the likelihood at $f_{\rm AGN} = 1$ and the one at $f_{\rm AGN} = 0$ for each GW event, as a function of the corresponding V90. Each panel shows the results for a different bolometric luminosity threshold. In each plot, the markers are coloured as a function of the average completeness of $\mathrm{Quaia}_{\rm cut}$ in the region occupied by V90. The dashed horizontal lines mark where $\mathcal{L}_i\,(f_{\rm AGN} = 1)\,/\mathcal{L}_i\,(f_{\rm AGN} = 0)$.

The main results of this work are summarised in Figure 5.5 and in Table 5.3. In particular we estimate that no more than the 21 per cent of the detected GW events used in our analysis originated from an AGN with a bolometric luminosity higher than $10^{44.5}$erg s^1. Objects brighter than such threshold consist of almost the entirety of the catalogue we consider. Due to the flux limitations of Quaia, fainter objects are not included in our analysis.

We find a particular GW event for which the single-event likelihood function suggests a possible AGN origin, especially when objects brighter than 10^{46}erg s^1 are considered. The ID of such event is S240511i, and it has been detected during O4b. Since the statistical framework used in this work is focused on analysing the entire population of GW events, the results concerning this specific event are to be considered as hints, not as statistically significant conclusions. Follow-up analyses, conducted especially when the full catalogue of mergers detected during O4 will we published, will be necessary to confidently assess whether or not this merger has an AGN origin.

Thanks to the increase of a factor ≈ 5 in the number of used GW events with respect to (Veronesi et al. 2023b) we are able to put much tighter constraints on the efficiency of the AGN channel (see Figure 5.5 for a comparison with our previous work). However, our results have been obtained under some assumptions, which are inevitable when inferring the properties of AGN in large catalogues. First and foremost, in order to calculate the bolometric luminosities of the Objects of Quaia we have to assume a shape of the typical SED and a value for the bolometric correction. We take the values of these AGN properties from Richards et al. (2006) in order to be consistent with what has been done in Wu & Shen (2022), which we use to adjust the bolometric luminosity obtained from Gaia magnitudes. Different assumptions on the SED and on the bolometric correction might lead to different estimates of the bolometric luminosities, even if these difference are not expected to be significant for our statistical analysis.

One more assumption is to be made during the calculation of the completeness of Quaia$_{\rm cut}$. This is in fact done comparing the observed number of AGN with the expected one, which obtained from the integration of a luminosity function. The best fit parameters of these functions depend on the data used during the fit, and different works might assume different analytical expression for them. We choose to use the luminosity function from Kulkarni et al. (2019) because in the redshift range considered in our analysis it has been fitted on AGN from SDSS, which is a survey that contains un-obscured AGN detectable in the optical band, like the ones contained in Quaia. Moreover, the objects contained in Wu & Shen (2022), used to obtain the final estimate on the bolometric luminosity of the objects in Quaia$_{\rm cut}$, come from SDSS. Comparing the

measured number of objects in the used AGN catalogue with a different luminosity function might lead to different estimates of its completeness, and the constraining power presented in this work is expected to scale linearly with such a parameter.

Another important caveat to mention is that our analysis and the constraints we are able to put concern un-obscured AGN, which are visible both in the optical and in the infrared band. In order to extend our conclusions to the entire population of AGN, one should take into account what fraction of them is not visible in the wavelength observed by Gaia and by WISE, which are the two surveys from which Quaia has been created from. This obscuration fraction, is in general expected to increase as a function of redshift and decrease as a function of luminosity (Merloni et al. 2014; Ueda et al. 2014).

The observational constraints presented in this work consist of a generalisation of the ones obtained in Veronesi et al. (2023b). Here we investigate a wider range of AGN luminosities and the entirety of the redshift range reached by the interferometers of the LVK collaboration. For this reason, in order to obtain in the future even more general results we need an all-sky AGN catalogue with a lower threshold in flux with respect to Quaia, in order to extend our analysis to the faint-end of the un-obscured AGN population. While we estimate that no more than one GW event out of five has originated in an un-obscured AGN with a bolometric luminosity higher than $10^{44.5}$erg s^1, a more significant fraction might come from fainter objects, or obscured ones.

While the results of this work demonstrate that the efficiency of the AGN channel can already be investigated with spatial-correlation analyses using the currently available data, tighter constraints will be possible to put in the next years, using all the events that will be detected in the rest of O4 as well as the ones that will be detected during the fifth observing run of the LVK collaboration, O5. Using more data could either reduce the upper limits on $f_{\rm AGN}$, or it could cause a shifting of the value of such parameter that maximised the posterior distribution, moving it away from zero.

Future developments of the statistical method used in this work involve also the introduction of physically-motivate priors on the intrinsic binary properties. Different binary formation channels are indeed expected to produce different features in the distributions of the masses and the spins of the merging systems, as well as on their eccentricity. The analysis here presented has been kept purposely agnostic as far as the physics of the formation mechanism is concerned. Introducing physically-motivated changes in the likelihood function might result in different constraints on $f_{\rm AGN}$ and will inform us on which are the intrinsic binary parameters that are able to add more information to the analysis.

Acknowledgements

EMR acknowledges support from ERC Grant "VEGA P.", number 101002511. This research has made use of data or software obtained from the Gravitational Wave Open Science Center (gwosc.org), a service of LIGO Laboratory, the LIGO Scientific Collaboration, the Virgo Collaboration, and KAGRA. LIGO Laboratory and Advanced LIGO are funded by the United States National Science Foundation (NSF) as well as the Science and Technology Facilities Council (STFC) of the United Kingdom, the Max-Planck-Society (MPS), and the State of Niedersachsen/Germany for support of the construction of Advanced LIGO and construction and operation of the GEO600 detector. Additional support for Advanced LIGO was provided by the Australian Research Council. Virgo is funded, through the European Gravitational Observatory (EGO), by the French Centre National de Recherche Scientifique (CNRS), the Italian Istituto Nazionale di Fisica Nucleare (INFN) and the Dutch Nikhef, with contributions by institutions from Belgium, Germany, Greece, Hungary, Ireland, Japan, Monaco, Poland, Portugal, Spain. KAGRA is supported by Ministry of Education, Culture, Sports, Science and Technology (MEXT), Japan Society for the Promotion of Science (JSPS) in Japan; National Research Foundation (NRF) and Ministry of Science and ICT (MSIT) in Korea; Academia Sinica (AS) and National Science and Technology Council (NSTC) in Taiwan. *Software*: `Numpy` (Harris et al. 2020); `Matplotlib` (Hunter 2007); `SciPy` (Virtanen et al. 2020); `Astropy` (Astropy Collaboration et al. 2013, 2018); `Bilby` (Ashton et al. 2019); `BAYESTAR` (Singer & Price 2016); `Healpy` (Zonca et al. 2019).

Data Availabilty

The data underlying this article will be shared on reasonable request to the corresponding author.

Bibliography

Aarseth S. J., Heggie D. C., 1976, A&A, 53, 259
Abbott B. P., et al., 2016, Phys. Rev. Lett., 116, 061102
Abbott B. P., et al., 2017, Physical Review Letters, 119, 161101
Abbott B. P., et al., 2018, Living Reviews in Relativity, 21, 3
Abbott B. P., et al., 2019, Physical Review X, 9, 031040
Abbott B. P., et al., 2020, Living Reviews in Relativity, 23, 3
Abbott R., et al., 2021a, Physical Review X, 11, 021053
Abbott R., et al., 2021b, SoftwareX, 13, 100658
Abbott R., et al., 2021c, ApJ, 913, L7
Abbott R., et al., 2023a, Physical Review X, 13, 011048
Abbott R., et al., 2023b, Physical Review X, 13, 041039
Abbott R., et al., 2023c, Physical Review X, 13, 041039
Abbott R., et al., 2023d, ApJS, 267, 29
Abbott R., et al., 2024a, Physical Review D, 109, 022001
Abbott R., et al., 2024b, Physical Reviews D, 109, 022001
Abdurro'uf et al., 2022, ApJS, 259, 35
Acernese F., et al., 2015, Classical and Quantum Gravity, 32, 024001
Ahumada R., et al., 2020, ApJS, 249, 3
Ajith P., et al., 2011, Phys. Rev. Lett., 106, 241101
Akutsu T., et al., 2021, Progress of Theoretical and Experimental Physics, 2021, 05A101
Alfradique V., et al., 2024, MNRAS, 528, 3249
Amaro-Seoane P., et al., 2017, arXiv e-prints, p. arXiv:1702.00786
Antoni A., MacLeod M., Ramirez-Ruiz E., 2019, ApJ, 884, 22
Antonini F., Rasio F. A., 2016, ApJ, 831, 187
Antonini F., Gieles M., Gualandris A., 2019, MNRAS, 486, 5008
Armitage P. J., 2007, arXiv e-prints, pp astro–ph/0701485
Armitage P. J., 2010, Astrophysics of Planet Formation
Ashton G., et al., 2019, Astrophys. J. Suppl., 241, 27
Ashton G., Ackley K., Hernandez I. M., Piotrzkowski B., 2021, Classical and Quantum Gravity, 38, 235004
Aso Y., Michimura Y., Somiya K., Ando M., Miyakawa O., Sekiguchi T., Tatsumi D., Yamamoto H., 2013, Physical Reviews D, 88, 043007
Assef R. J., et al., 2013, ApJ, 772, 26
Astropy Collaboration et al., 2013, A&A, 558, A33
Astropy Collaboration et al., 2018, AJ, 156, 123
Barrera O., Bartos I., 2022, ApJ, 929, L1

Bartos I., 2016a, in American Astronomical Society Meeting Abstracts #228. p. 208.03
Bartos I., 2016b, in American Astronomical Society Meeting Abstracts #228. p. 208.03
Bartos I., Haiman Z., Marka Z., Metzger B. D., Stone N. C., Marka S., 2017a, Nature Communications, 8, 831
Bartos I., Haiman Z., Marka Z., Metzger B. D., Stone N. C., Marka S., 2017b, Nature Communications, 8, 831
Bartos I., Kocsis B., Haiman Z., Márka S., 2017c, ApJ, 835, 165
Bekenstein J. D., 1973, ApJ, 183, 657
Bekki K., Couch W. J., Shioya Y., Vazdekis A., 2005, MNRAS, 359, 949
Belczynski K., et al., 2016, A&A, 594, A97
Belczynski K., Doctor Z., Zevin M., Olejak A., Banerje S., Chattopadhyay D., 2022, ApJ, 935, 126
Bellm E. C., et al., 2019a, PASP, 131, 018002
Bellm E. C., et al., 2019b, PASP, 131, 018002
Bellovary J. M., Mac Low M.-M., McKernan B., Ford K. E. S., 2016, ApJ, 819, L17
Binney J., Tremaine S., 2008, Galactic Dynamics: Second Edition
Blanton M. R., et al., 2017, AJ, 154, 28
Bonnor W. B., Rotenberg M. A., 1961, Proceedings of the Royal Society of London Series A, 265, 109
Bowyer S., Byram E. T., Chubb T. A., Friedman H., 1965, Science, 147, 394
Braun J., Dumm J., De Palma F., Finley C., Karle A., Montaruli T., 2008, Astroparticle Physics, 29, 299
Calcino J., Dempsey A. M., Dittmann A. J., Li H., 2023a, arXiv e-prints, p. arXiv:2311.13727
Calcino J., Dempsey A. M., Dittmann A. J., Li H., 2023b, arXiv e-prints, p. arXiv:2311.13727
Callister T. A., Haster C.-J., Ng K. K. Y., Vitale S., Farr W. M., 2021, ApJ, 922, L5
Campanelli M., Lousto C. O., Zlochower Y., Merritt D., 2007, Phys. Rev. Lett., 98, 231102
Chandrasekhar S., 1943, ApJ, 97, 255
Chattopadhyay D., Stegmann J., Antonini F., Barber J., Romero-Shaw I. M., 2023, MNRAS, 526, 4908
Chen K., Dai Z.-G., 2024, ApJ, 961, 206
Colless M., et al., 2001, MNRAS, 328, 1039
Corley K. R., et al., 2019, MNRAS, 488, 4459